New Iterative Perturbation Scheme for Lattice Models with Arbitrary Filling

Henrik Kajueter and Gabriel Kotliar
Department of Physics, Rutgers University, Piscataway, New Jersey 08855-0849
(Received 25 September 1995)

We derive a new perturbation scheme for treating the large d limit of lattice models at arbitrary filling. The results are compared with exact diagonalization data for the Hubbard model and found to be in good agreement. [S0031-9007(96)00438-3]

PACS numbers: 71.30.+h, 71.10.Fd, 71.27.+a, 74.20.Mn

In recent years there has been a renewed interest in the study of strongly correlated electron materials. These materials exhibit interesting phenomena like the correlation induced metal insulator transition [1–3]. A very promising method capable of providing a theoretical description, perhaps, is the limit of large spatial dimensions [4], which defines a dynamical mean field theory for the problem. This limit can be mapped onto an impurity model together with a self-consistency condition which is characteristic for the specific model under consideration [5]. The mapping allows one to apply several numerical and analytical techniques which have been developed to analyze impurity models over the years. There are different approaches which have been used for this purpose: qualitative analysis of the mean field equations [5], quantum Monte Carlo methods [6–8], iterative perturbation theory (IPT) [5,9], exact diagonalization methods [10,11], and the projective self-consistent method, a renormalization technique [12]. However, each of these methods has its shortfalls. While quantum Monte Carlo calculations are not applicable in the zero temperature limit, the exact diagonalization methods and the projective self-consistent method yield only a discrete number of poles for the density of states. Moreover, the computational requirements of the exact diagonalization and the quantum Monte Carlo methods are such that they can only be implemented for the simplest Hamiltonians. To carry out realistic calculations it is necessary to have an accurate but fast algorithm for solving the impurity model. In this context iterative perturbation theory has turned out to be a useful and reliable tool for the case of half filling [13,14]. However, for finite doping the naive extension of the IPT scheme is known to give unphysical results. There is still no method which can be applied away from half filling and which at the same time is powerful enough to treat more complicated models.

The aim of this paper is to close this gap by introducing a new iterative perturbation scheme which is applicable at arbitrary filling.

The (asymmetric) Anderson impurity model

$$H_{\mathrm{imp}} = \epsilon_f \sum_{\sigma} f_{\sigma}^{\dagger} f_{\sigma} + \sum_{k,\sigma} \epsilon_k c_{k\sigma}^{\dagger} c_{k\sigma} + \sum_{k,\sigma} V_k (c_{k\sigma}^{\dagger} f_{\sigma} + f_{\sigma}^{\dagger} c_{k\sigma}) + U f_{\downarrow}^{\dagger} f_{\downarrow} f_{\uparrow}^{\dagger} f_{\uparrow} \tag{1}$$

describes an impurity (f_σ) coupled to a bath of conduction electrons ($c_{k\sigma}$). The hybridization function is given by $\Delta(\omega) = \sum_k [V_k^2/(\omega - \epsilon_k)]$. Once a solution is known for arbitrary parameters a large number of lattice models can be solved by iteration. An example is the Hubbard Hamiltonian,

$$H = -\frac{t}{\sqrt{z}} \sum_{\langle ij\rangle,\sigma} c_{i\sigma}^{\dagger} c_{j\sigma} + U \sum_i n_{i\uparrow} n_{i\downarrow}, \tag{2}$$

which can actually serve as an effective Hamiltonian for the description of doped transition metal oxides [15]. On a Bethe lattice with infinite coordination number z the Hubbard model is connected to the impurity model by the following self-consistency condition:

$$\Delta(\omega) = t^2 G(\omega) \tag{3}$$

and $\epsilon_f = -\mu$. The mapping requires that the propagator of the lattice problem is given by the impurity Green function ($G = G_f$). We set $D := 2t = 1$.

Below we derive the perturbation scheme for the impurity model. Afterwards the scheme is applied to the Hubbard model. Some results for the doped system are presented, and the accuracy of our scheme is discussed. We conclude with a summary and an outlook.

Derivation of the approximation scheme for the single impurity model.—Here we derive the approximation scheme which, given the hybridization function $\Delta(\omega)$ and the impurity level ϵ_f, provides a solution of model (1). For simplicity, we assume that there is no magnetic symmetry breaking ($n_\sigma = n_{-\sigma} = n$). We also restrict us to zero temperature. The procedure is an extension of the ordinary IPT scheme to finite doping. The success of IPT at half filling can be explained by the fact that it becomes exact not only in the weak but also in the strong coupling limit [13]. Moreover, this approach captures the right low and high frequency behavior so that we are dealing with an interpolation scheme between correct limits.

The idea of our approach is to construct a self-energy expression which retains these features at arbitrary doping and reduces at half filling to the ordinary IPT result.

Ordinary IPT approximates the self-energy by its second order contribution, $\sum(\omega) \approx Un + \tilde{\sum}_0^{(2)}(\omega)$, where

$$\tilde{\Sigma}_0^{(2)}(\omega) := U^2 \int_{-\infty}^{0} d\epsilon_1 \int_0^{\infty} d\epsilon_2\, d\epsilon_3\, \frac{\rho^{(0)}(\epsilon_1)\rho^{(0)}(\epsilon_2)\rho^{(0)}(\epsilon_3)}{\omega + \epsilon_1 - \epsilon_2 - \epsilon_3 - i\eta} + U^2 \int_0^{\infty} d\epsilon_1 \int_{-\infty}^{0} d\epsilon_2\, d\epsilon_3\, \frac{\rho^{(0)}(\epsilon_1)\rho^{(0)}(\epsilon_2)\rho^{(0)}(\epsilon_3)}{\omega + \epsilon_1 - \epsilon_2 - \epsilon_3 - i\eta}, \tag{4}$$

with $\rho^{(0)} = (1/\pi)\mathrm{Im}G_0$. Here, the (advanced) Green function $G_0(\omega)$ is defined by

$$G_0(\omega) := \frac{1}{\omega + \tilde{\mu}_0 - \Delta(\omega)}. \tag{5}$$

The parameter $\tilde{\mu}_0$ is given by $-\epsilon_f - Un$. In particular, it vanishes at half filling. The full Green function follows from

$$G_f(\omega) = \frac{1}{G_0^{-1} - \tilde{\mu}_0 - \epsilon_f - \sum(\omega)}. \tag{6}$$

To ensure the correctness of this approximation scheme in different limits, we modify the self-energy functional as well as the definition of the parameter $\tilde{\mu}_0$.

We start with an ansatz for the self-energy,

$$\sum_{\mathrm{int}}(\omega) = Un + \frac{A\tilde{\Sigma}_0^{(2)}(\omega)}{1 - B\tilde{\Sigma}_0^{(2)}(\omega)}. \tag{7}$$

Here $\tilde{\Sigma}_0^{(2)}(\omega)$ is the normal second order contribution defined in Eq. (4). We determine the parameter A from the condition that the self-energy has the exact behavior at high frequencies. Afterwards, B is determined from the atomic limit.

The leading behavior for large ω can be obtained by expanding the Green function into a continuous fraction [16]: $G_f(\omega) = 1/[\omega - \epsilon_f - \alpha_1 - (\alpha_2 - \alpha_1^2)/(\omega + \cdots)]$. Here, α_i marks the ith order moment of the density of states. One can compute these quantities by evaluating a commutator (see [17]). We obtain for our model $G_f(\omega) = 1/\{\omega - \epsilon_f - Un - [\sum_k V_k^2 + U^2 n(1-n)]/(\omega + \cdots)\}$. The leading term of the self-energy is therefore given by

$$\sum(\omega) = Un + U^2 n(1-n)\frac{1}{\omega} + O\left(\left(\frac{1}{\omega}\right)^2\right). \tag{8}$$

Here n is the physical particle number given by $n = \int_{-\infty}^{0} d\omega\, \mathrm{Im}G_f(\omega)$. Equation (8) has to be compared with the large frequency limit of (4),

$$\tilde{\Sigma}_0^{(2)}(\omega) = U^2 n_0(1-n_0)\frac{1}{\omega} + O\left(\left(\frac{1}{\omega}\right)^2\right), \tag{9}$$

where n_0 is a fictitious particle number determined from G_0 [i.e., $n_0 = \int_{-\infty}^{0} d\omega\, \mathrm{Im}G_0(\omega)$]. From (7), (8), and (9) we conclude

$$A = \frac{n(1-n)}{n_0(1-n_0)}. \tag{10}$$

Choosing A in this way guarantees that our self-energy is correct to order $1/\omega$. It should be noted from the continuous fraction considered above that, consequently, the moments of the density of states up to second order are reproduced exactly.

Next, we have to fix B. The exact impurity Green function for $V_k \to 0$ is given by [18]

$$G_f(\omega) = \frac{n}{\omega - \epsilon_f - U - i\eta} + \frac{1-n}{\omega - \epsilon_f - i\eta}. \tag{11}$$

This can be written as $G_f(\omega) = 1/[\omega - \epsilon_f - \sum_{\mathrm{atomic}}(\omega)]$ where

$$\sum_{\mathrm{atomic}}(\omega) = Un + \frac{n(1-n)U^2}{\omega - \epsilon_f - (1-n)U - i\eta}. \tag{12}$$

This expression is to be compared with the atomic limit of our ansatz (7). Since $\tilde{\Sigma}_0^{(2)}(\omega) \to U^2 n_0(1-n_0)/(\omega + \tilde{\mu}_0 - i\eta)$, we obtain

$$B = \frac{(1-n)U + \epsilon_f + \tilde{\mu}_0}{n_0(1-n_0)U^2}. \tag{13}$$

Thus, the final result for our interpolating self-energy is

$$\sum_{\mathrm{int}}(\omega) = Un + \frac{[n(1-n)/n_0(1-n_0)]\tilde{\Sigma}_0^{(2)}(\omega)}{1 - \{[(1-n)U + \epsilon_f + \tilde{\mu}_0]/n_0(1-n_0)U^2\}\tilde{\Sigma}_0^{(2)}(\omega)}. \tag{14}$$

Yet $\tilde{\mu}_0$ is still a free parameter. We fix it imposing the Friedel sum rule [19],

$$n = \frac{1}{2} - \frac{1}{\pi}\arctan\left(\frac{\epsilon_f + \sum_{\mathrm{int}}(0) + \mathrm{Re}\Delta(0)}{\mathrm{Im}\Delta(0)}\right) + \int_{-i\infty}^{+i\infty} \frac{d\omega}{2\pi i} G_f(\omega)\frac{\partial\Delta(\omega)}{\partial\omega}. \tag{15}$$

This statement, which is equivalent to the Luttinger theorem [20] $\int_{-i\infty}^{+i\infty}(d\omega/2\pi i)G_f(\omega)(\partial\sum_{\mathrm{int}}(\omega)/\partial\omega) = 0$, should be viewed as a condition on the zero frequency value of the self-energy to obtain the correct low energy behavior. The use of the Friedel sum rule is the main difference to earlier approximation schemes [21–23] and

is essential to obtain a good agreement with the exact diagonalization method.

So far, we considered three different limits: strong coupling, zero frequency, and large frequency. It remains to check the weak coupling limit. Taking into account that $n = n_0$ and $\tilde{\mu}_0 = -\epsilon_f$ for $U = 0$, it follows that (14) is indeed exact to order U^2.

The actual solution of the impurity model is determined by a pair $(\tilde{\mu}_0, n)$ which satisfies Eqs. (4), (5), (6), (14), and (15). For the numerical implementation Broyden's method [24], a generalization of Newton's method, has turned out to be very powerful. Defining two functions $f_1(n, \tilde{\mu}_0) := n - \int_{-\infty}^{0} d\omega \, \mathrm{Im}G_f[n, \tilde{\mu}_0](\omega)$ and $f_2(n, \tilde{\mu}_0) := n - n_{\mathrm{Friedel}}[n, \tilde{\mu}_0]$ the impurity problem can be solved by searching for the zeros of f_1 and f_2 (n_{Friedel} is the particle number determined from the Friedel sum rule). The algorithm is very efficient as in most cases a solution is found within 4 to 10 iterations.

Application to the Hubbard model.—After treating the Anderson impurity model, we now apply the perturbation scheme to the solution of the Hubbard model. Starting with a guess for $\Delta(\omega)$ one can solve the impurity model using the scheme described above. This yields a propagator $G_f = G$, which can be used to determine a new hybridization function $\Delta(\omega)$ according to (3). The iteration is continued until convergence is attained. It is most accurate to perform the calculation first on the imaginary axis. Once the constants A and B in the interpolating self-energy are determined in this way, they can be used to perform the iteration on the real axis.

In the case of the Hubbard model, the Luttinger theorem takes the simple form [25]

$$\mu_0 = \mu - \sum_{\mathrm{int}}(\omega = 0), \quad \mu_0 := \mu|_{U=0}. \tag{16}$$

This can be used to simplify the self-consistency procedure if $\tilde{\mu}_0$ rather than μ is fixed. Starting with a guess for G and μ, one can compute G_0, n, and n_0. Afterwards (14) yields $\sum_{\mathrm{int}}(\omega)$ and a new μ is obtained from (16).

To illustrate the accuracy of our method we compare it with results obtained using the exact diagonalization algorithm of Caffarel and Krauth [10] for 8 sites. Both methods are in close agreement when used on the imaginary axis: As far as $\mathrm{Im}G(i\omega)$ is concerned, the deviations between both methods are only about 1% so that the curves can hardly be distinguished. The real advantage of our perturbation scheme compared to the exact diagonalization is disclosed when we display the spectra functions obtained by these two methods on the real axis (Fig. 1).

It is clear that the exact diagonalization is doing its best in producing the correct spectral distribution. But it is unable to give a smooth density of states. Instead several sharp structures occur as a consequence of treating only a finite number of orbitals in the Anderson model.

To obtain a more meaningful comparison on the real axis, we plotted in Fig. 2 the integrated spectral weight $F(\omega) := (1/\pi)\int_{-\infty}^{\omega} d\tilde{\omega}\mathrm{Im}G(\tilde{\omega})$ as obtained from exact

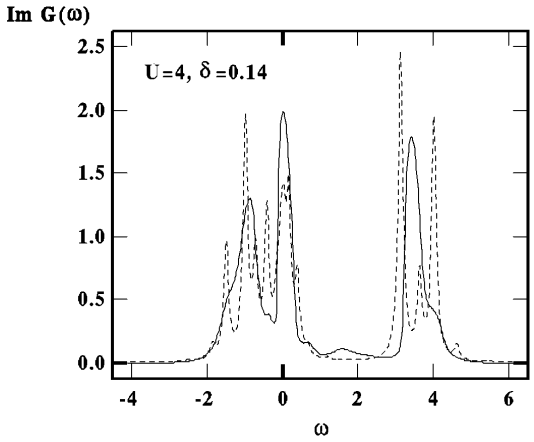

FIG. 1. $\mathrm{Im}G(\omega)$ at $T = 0$ for $U = 4D$ and hole doping $\delta = 0.14$: iterative perturbation scheme (full line) vs exact diagonalization (8 sites, dashed line).

diagonalization and our perturbation scheme. We find a good agreement between both methods.

Similar to the half filled Hubbard model [7] it can be shown that for large U there is a Mott transition. Figure 3 shows the evolution of the spectral density of the doped Mott insulator ($U = 4D$) with increasing hole doping δ. The qualitative features are those expected from the spectra of the single impurity [5] and are in agreement with the quantum Monte Carlo calculations [26]. For small doping there is a clear resonance peak at the Fermi level. Its width is given by the quasiparticle residue Z which near the Mott transition behaves like $Z \sim \mu_c - \mu$. As δ is increased, the peak broadens and is shifted through the lower Hubbard band. At the same time the weight of the upper band decreases.

The most striking feature of the evolution of the spectral density as a function of doping is the finite shift of the Kondo resonance from the insulating band edge as the doping goes to zero. It was demonstrated analytically that this is a genuine property of the exact solution of the Hubbard model in infinite dimensions using the projective

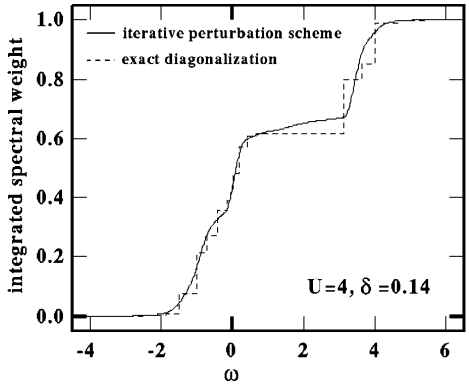

FIG. 2. Integrated spectral weight for $U = 4D$ and hole doping $\delta = 0.14$: iterative perturbation scheme (full line) vs exact diagonalization (8 sites, dashed line).

self-consistent method [27] and is one of the most striking properties of the Hubbard model in large dimensions. This feature did not appear in the earlier studies of Hubbard model in large dimensions using Monte Carlo techniques [26] at higher temperatures, and is also not easily seen in exact diagonalization algorithms [15].

In this paper we introduced a new perturbation scheme for the solution of lattice models away from half filling. The basic idea is to construct an expression for the self-energy which interpolates between correct limits. In the weak coupling limit our approximate self-energy is exact to order U^2, and it is also exact in the atomic limit. The proper low frequency behavior is ensured by the Friedel sum rule (or, equivalently, the Luttinger theorem). This is important to obtain the right low energy features in the spectral density. The overall distribution of the density of states, on the other hand, is determined by the spectral moments, which are reproduced exactly up to second order by satisfying the proper large frequency behavior. More important our results are in very good agreement with the exact diagonalization method and allowed us to obtain explicit results for the evolution of the spectral function as a function of doping.

Since the algorithm described here is accurate and very fast (a typical run to solve the Hubbard model takes 60 sec on a DEC alpha station 200 4/233), it has a wide range of applications. Two examples that come to mind are the effects of disorder on the Hubbard model away from half filling and the study of realistic models with orbital degeneracy. The latter is very important to make contact with realistic three dimensional transition metal oxides.

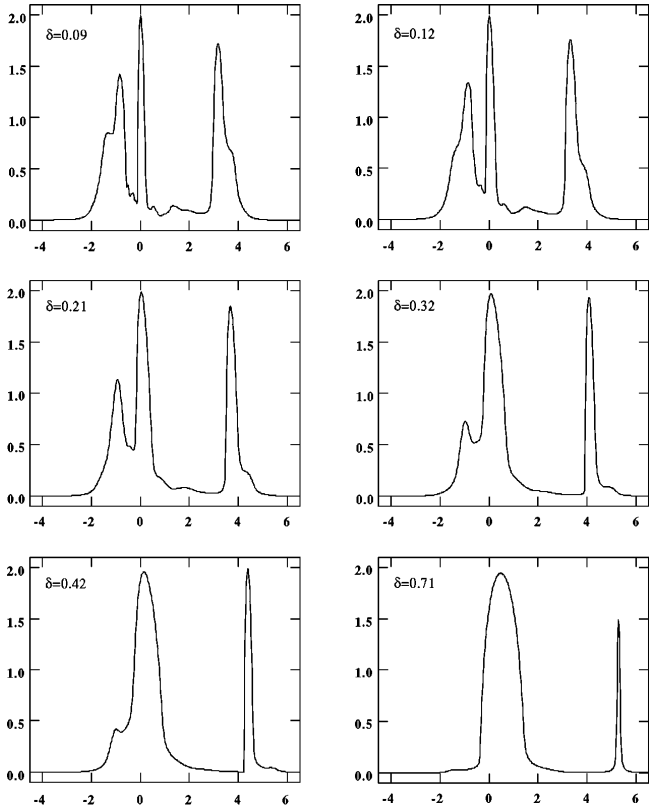

FIG. 3. Evolution of the spectral function for $U = 4D$ and $T = 0$ with increasing hole doping δ.

This work has been supported by the National Science Foundation, DMR 95-29138.

[1] Y. Tokura, Y. Taguchi, Y. Okada, Y. Fujishima, T. Arima, K. Kumagai, and Y. Iye, Phys. Rev. Lett. **70**, 2126 (1993).
[2] Y. Okimoto, T. Katsufuji, and Y. Tokura, Phys. Rev. B **51**, 9581 (1995).
[3] T. Katsufuji, Y. Okimoto, and Y. Tokura (to be published).
[4] W. Metzner and D. Vollhardt, Phys. Rev. Lett. **62**, 324 (1989).
[5] A. Georges and G. Kotliar, Phys. Rev. B **45**, 6479 (1992).
[6] M. Jarrell, Phys. Rev. Lett. **69**, 168 (1992).
[7] M. Rozenberg, X. Y. Zhang, and G. Kotliar, Phys. Rev. Lett. **69**, 1236 (1992).
[8] A. Georges and W. Krauth, Phys. Rev. Lett. **69**, 1240 (1992).
[9] X. Y. Zhang, M. J. Rozenberg, and G. Kotliar, Phys. Rev. Lett. **70**, 1666 (1993).
[10] M. Caffarel and W. Krauth, Phys. Rev. Lett. **72**, 1545 (1994); Q. Si, M. Rozenberg, G. Kotliar, and A. Ruckenstein, Phys. Rev. Lett. **72**, 2761 (1994).
[11] A. Georges and W. Krauth, Phys. Rev. B **48**, 7167 (1993).
[12] G. Moeller, Q. Si, G. Kotliar, M. Rozenberg, and D. S. Fisher, Phys. Rev. Lett. **74**, 2082 (1995).
[13] M. J. Rozenberg, G. Kotliar, and X. Y. Zhang, Phys. Rev. B **49**, 10 181 (1994).
[14] M. J. Rozenberg, G. Kotliar, H. Kajueter, G. A. Thomas, D. H. Rapkine, J. M. Honig, and P. Metcalf, Phys. Rev. Lett. **75**, 105 (1995).
[15] H. Kajueter, G. Kotliar, and G. Moeller, Phys. Rev. B (to be published).
[16] R. G. Gordon, J. Math. Phys. (N.Y.) **9**, 655 (1968).
[17] W. Nolting and W. Borgie, Phys. Rev. B **39**, 6962 (1989).
[18] W. Brenig and K. Schönhammer, Z. Phys. **267**, 201 (1974).
[19] D. C. Langreth, Phys. Rev. **150**, 516 (1966).
[20] J. M. Luttinger and J. C. Ward, Phys. Rev. **118**, 1417 (1960).
[21] A. Martin-Rodero, F. Flores, M. Baldo, and R. Pucci, Solid State Commun. **44**, 911 (1982).
[22] D. M. Edwards and J. A. Hertz, Physica (Amsterdam) **163B**, 527 (1990).
[23] W. Wermbter and G. Czycholl, J. Phys. Condens. Mater **7**, 7335 (1995).
[24] W. H. Press *et al.*, *Numerical Recipes in Fortran* (Cambridge Press, Cambridge, 1992), 2nd ed., p. 382.
[25] E. Müller-Hartmann, Z. Phys. B **76**, 211 (1989).
[26] M. Jarrell and T. Pruschke, Z. Phys. B **90**, 187 (1993).
[27] D. Fisher, G. Kotliar, and G. Moeller, Phys. Rev. B **52**, 1712 (1995).